



*Anal. Bioanal. Chem. Res., Vol. 7, No. 2, 251-262, June 2020.*

## **Preparation of Silicagel-MnO<sub>2</sub> Nanocomposite Adsorbent for Malachite Green Removal**

Sayed Zia Mohammadi<sup>a,\*</sup>, Maryam Sharifimehr<sup>a</sup>, Farideh Mosazadeh<sup>b</sup> and Nastaran Mofidinasab<sup>a</sup>

<sup>a</sup>*Department of Chemistry, Payame Noor University, Tehran, Iran*

<sup>b</sup>*School of Public Health, Bam University of Medical Sciences, Bam, Iran*

*(Received 18 May 2019 Accepted 7 January 2020)*

Silicagel-MnO<sub>2</sub> (Si-MnO<sub>2</sub>) nanocomposite has been prepared by co-precipitation method and characterized using SEM, XPS and FT-IR techniques. Adsorption behavior of malachite green (MG) dye onto the prepared Si-MnO<sub>2</sub> has been examined and optimized. The batch procedure has been used for sorption kinetic and equilibrium examinations. The experiments have been done with an initial concentration of 100 mg l<sup>-1</sup> at room temperature. The representation of the equilibrium data is fully assessed via Freundlich and Langmuir isotherms. With regard to the Langmuir model, the greatest adsorption capacity of MG dye onto Si-MnO<sub>2</sub> was found to be 107.5 mg g<sup>-1</sup>, at room temperature. Kinetic examinations revealed that adsorption procedure follows pseudo-first-order model. Based on the results, prepared Si-MnO<sub>2</sub> could be economically and efficiently used as an adsorbent to remove MG dye from wastewater samples. Desorption of dye has been done using 0.1 M HCl solution and regenerated Si-MnO<sub>2</sub> can be used for five cycles of MG dye adsorption.

**Keywords:** Adsorption, Malachite green, Modified silicagel, MnO<sub>2</sub> nanoparticles

### **INTRODUCTION**

Recently, the main environmental and human health concern is water pollution [1,2]. Today, dyes hurt a lot of living organisms [3,4]. Longer exposure to water contaminated by metal ions and dyes subsequently influence human health and induce unfavorable problems for natural ecosystems [5,6]. A majority of dyes have stability to heat, light, and oxidation agents [7,8]. They hurt both aquatic life and human because of their poisonousness and capability to become a carcinogenic or mutagenic agent [7,9,10]. Malachite green (MG) has a widespread application in cotton wool, paper, leather, and silk industries as well as a treatment agent for treating fungal, bacterial, and parasite infections [11,12]. In spite of the intensive application of MG, it can act as a carcinogenicity, teratogenicity, mutagenicity, and respiratory poisonousness agent [13,14]. Hence, discovering efficient techniques for

removing dyes from effluents is of crucial importance. In order to treat waste water, electrochemical, membrane separation, biological oxidation, absorption, and ion exchanges methods have been developed. Because of simpleness, cost-effectiveness, and favorable procedures, adsorption is a suitable option for separating a variety of pollutants from industrial effluents [11,15,16]. This method forms no dangerous materials. Recently, different substances were applied to remove dyes from aqueous solutions [17-33]. In recent years, nano-materials are fascinating and efficient adsorbents to remove dyes due to their attractive chemical and physical features that increase adsorption efficacy to eliminate dyes [34-37].

Although silica gel is a sorbent with a highly interesting benefits, it should be modified with metals, metal oxide or another substances for enhancing adsorption potential toward dye molecules [38,39]. For this purpose, metal oxides were employed to modify the silica gel surface that might increase adsorption and catalytic properties. The obtained data from previous works showed that the nano-

\*Corresponding author. E-mail: szmohammadi@yahoo.com

sized metal oxides (*e.g.*, aluminum oxide, manganese oxide, titanium oxide, & ferric oxide) are useful for removal of pollutants from effluents because of their affinity toward impurities and higher surface areas/volume [39]. As adsorbent, MnO<sub>2</sub> has had a widespread usage as an efficient adsorbent to remove dyes from aqueous solution because of its higher adsorption capacities and selectivity [40].

In this work, the analytical potential of silica gel coated with MnO<sub>2</sub> (Si-MnO<sub>2</sub>) was examined for removal of MG from water samples. According to our information, Si-MnO<sub>2</sub> has been never employed before. Moreover, the impacts of initial adsorbate concentrations, contact time, pH, and capacities of sorbent on the MG removal were assessed.

## EXPERIMENTAL

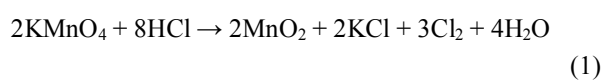
### Apparatus and Reagents

In order to measure absorbance, a varian scanning spectrophotometer (model CARY 50 Conc) with quartz cells has been used. Absorbance value of MG has been measured at 616 nm ( $\lambda_{\text{max}}$ ). A pH-meter (model: 827, Metrohm, Herisau, Switzerland) has been used to measure pH. A stirrer (model KS, IKA, Staufen, Germany) has been used for combination. A Centurion scientific centrifuge model 1020 D.E. (West Sussex, United Kingdom) has been employed for accelerating the stage separation. Its standard calibration curve has been used to achieve MG solution concentration.

All chemical compounds have the analytical-reagent grade and solutions have been procured with double distilled water. A stock solution of MG at a concentration of 1000.0  $\mu\text{g ml}^{-1}$  has been procured *via* dissolution of suitable amounts of MG (Merck, Darmstadt, Germany) in double distilled water. Working reference solutions have been gained every day by step-wise dilution.

### Preparation of Si-MnO<sub>2</sub>

Manganese dioxide was precipitated onto silicagel in aqueous solution by a reductive reaction (Eq. (1)) [41]:



To do so, 4.0 g potassium permanganate was taken in a beaker containing 50 ml deionized water and 4.0 g silicagel. Afterwards, eight ml concentrated HCl was added dropwise to it by continual stirring and heating on a hot plate at 90 °C. The heating and stirring was followed for 1 h. The coated silicagel was filtered, washed with boil water and dried at an oven at 80 °C for 6 h and stored in bottle for later uses.

### Characterizing the Procured Adsorbents

Scanning electron micrograph (SEM) (Cam Scan MV2300) has been used to observe Si-MnO<sub>2</sub> microstructures (Fig. 1). A thin layer of gold has been sputter-coated on sample to dissipate charges during SEM imaging. According to the figure, adsorbent possessed an irregular and porous surface that indicates partially higher surface areas.

Chemical characteristics of Si-MnO<sub>2</sub> have been examined via Fourier transform infrared (FT-IR) spectroscopy for identifying practical groups at Si-MnO<sub>2</sub> surface. Recording FT-IR spectra has been performed using a Bruker Tensor 27 spectrometer from 400 to 4000  $\text{cm}^{-1}$  through KBr wafer method. Wafers have been procured through mixing of 1 mg Si-MnO<sub>2</sub> and 100 mg of KBr. Figure 2 shows FT-IR spectra of the samples silica gel (a) and Si-MnO<sub>2</sub> (b). Absorption peaks appearing at 3670  $\text{cm}^{-1}$  have been ascribed to the stretching vibrations of hydroxyl groups at silica gel (a) and Si-MnO<sub>2</sub> (b) surfaces. The peak at 1660  $\text{cm}^{-1}$  is assigned to O-H stretching vibrations of adsorbed water. Moreover, absorption peak at 797  $\text{cm}^{-1}$  may be ascribed to Si-O symmetric stretching vibrations. FT-IR spectrum of Si-MnO<sub>2</sub> (b) revealed two novel adsorption peaks at 600 and 1440  $\text{cm}^{-1}$ . The former can be assigned to the Mn-O bending vibrations [42], while the latter has been attributed to the bending vibrations of -OH group bond to the Mn atoms [42].

X-ray photo-electron spectroscopy (XPS) has been done for characterizing chemical compositions of Si-MnO<sub>2</sub>. Figure 3 shows XPS spectrum of Si-MnO<sub>2</sub>. It depicts the existence of Mn, Si, and O elements in Si-MnO<sub>2</sub>. Weight ratios of Mn (40.35%), O (35.89%), and Si (23.76%) have been quantitatively analyzed.

Nitrogen absorption-desorption has been analyzed to study Brunauer-Emmett-Teller (BET) specific surface areas

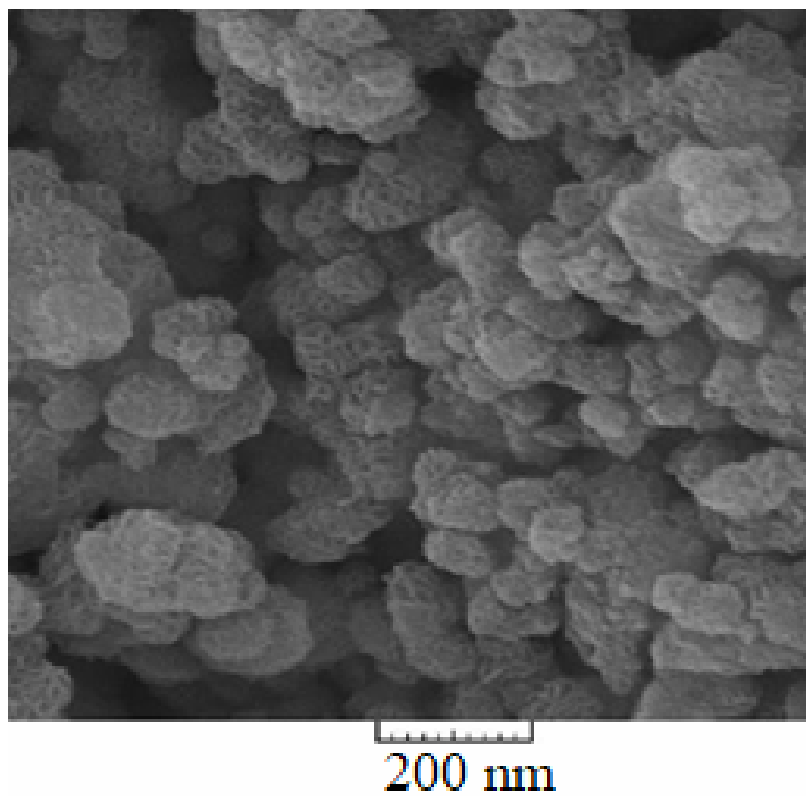


Fig. 1. SEM image of Si-MnO<sub>2</sub>.

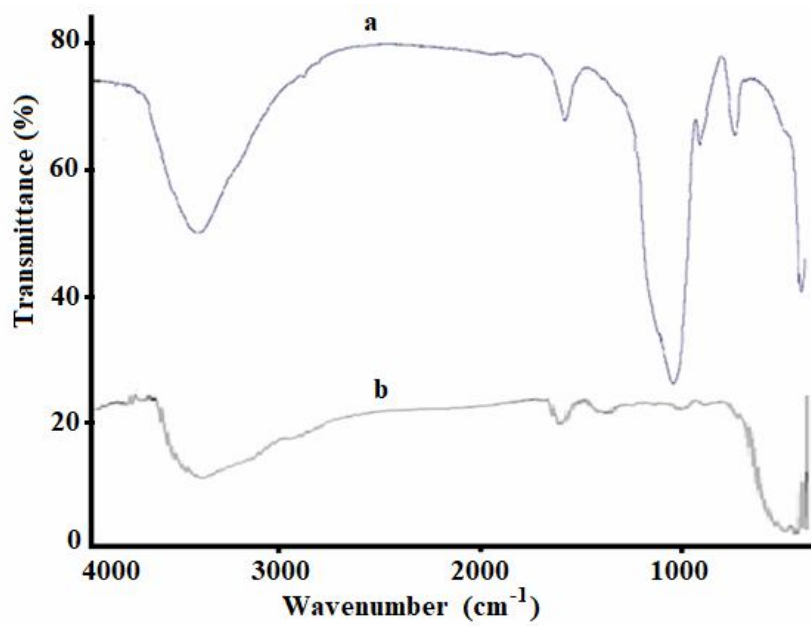


Fig. 2. Fourier transform infrared spectra of (a) silicagel, and (b) Si-MnO<sub>2</sub>.

of Si-MnO<sub>2</sub>. Outputs indicated that BET specific surface area of Si-MnO<sub>2</sub> is 387.4 m<sup>2</sup> g<sup>-1</sup>.

### Method of Experiments

Batch adsorption tests have been conducted by contacting 0.05 g of Si-MnO<sub>2</sub> with 20 ml of aqueous solution containing various initial concentrations (50-300 mg l<sup>-1</sup>) of MG at pH 6. Experiments have been done in 100 ml Erlenmeyer flasks. Agitation of the flasks has been done on an IKA stirrer model KS at 180 rpm for the time periods determined at room temperature. The residual concentrations of MG in all samples have been identified *via* spectrophotometer after centrifuging at 3000 rpm for five minutes. The MG concentration remained in the adsorbent stage has been computed based on Eq. (2).

$$q_e = v(C_0 - C_e) / m \quad (2)$$

where  $q_e$  (mg g<sup>-1</sup>) represents equilibrium amount of MG in the adsorption stage,  $C_0$  and  $C_e$  denote initial and equilibrium concentration of MG (mg l<sup>-1</sup>) in aqueous solutions,  $v$  implies the solution volume (l), and  $m$  represents the sorbent dosage (g) in the mix.

Equation (3) has been used to calculate the removal percentage of MG (Re%) from aqueous solutions.

$$\text{Re\%} = [(C_0 - C_e) / C_0] \times 100 \quad (3)$$

## RESULTS AND DISCUSSION

### The Impact of Solution Initial pH

One of the most prominent factors is pH affecting both dissociating site and MG solution chemistry.

For studying the impact of pH on the adsorption of MG by Si-MnO<sub>2</sub>, initial solution pH was changed at pH ranged from 2-8. The experiments have been done with an initial concentration of 100 mg l<sup>-1</sup> at room temperature. The results (Fig. 4) showed that the highest level of MG uptake was obtained at the pH range 6-8. This finding may be caused by the fact that the greater pHs lead to the higher deprotonation of adsorbent surfaces, which enhances negative charged locations suitable for electrostatic attraction between the surfaces of adsorbent and MG. The lower pHs lead to the greater positive charge sites enhancing the repulsion forces

between adsorbent surface and MG and reducing the potential of adsorption [43]. Therefore, pH 7 has been regarded for additional tests.

### Examining the Contact Time

Equilibration time is a parameter used for economical waste water treatment plants. The impact of contact time on adsorption of MG on Si-MnO<sub>2</sub> is depicted in Fig. 5. As can be seen in Fig. 5, more than 60% of MG has been adsorbed during the first 10 min. As time increases, sorption kinetics declines gradually. Ultimately, adsorption reached equilibrium within 30 min. Fast adsorption could be caused by rapid transferring of MG due to the impact of the related driving forces, including shaking and concentrations gradient on the active surface area of the adsorbent.

The trend in adsorption of MG dye indicates that adsorption may be *via* interaction with functional groups situated on the surface of Si-MnO<sub>2</sub>. With regard to the results, an agitation time of 30 min has been chosen for assuring the desirable equilibrium.

### The Impact of Initial Concentrations

The impact of initial concentration of MG dye on adsorption was examined. Therefore, one set of experiment has been conducted with different initial concentrations of MG (50-300 mg l<sup>-1</sup>) by using 0.05 g of adsorbent at pH 7. Fig. 6 and Table 1 shows the results. As initial concentration increases, the Re% declines, although real amounts of MG adsorbed per unit mass of Si-MnO<sub>2</sub> enhanced with increase in initial concentrations. At low concentrations, the ratio of MG to sorption sites onto surface of Si-MnO<sub>2</sub> is low and, therefore, the fractional adsorption becomes independent of initial concentration; whereas, at high concentrations, the existing sites of adsorption become lower and therefore the removal of MG depends on the initial concentrations. Therefore, removing MG dye is dependent on the initial concentrations and declines as the initial MG concentration increases.

### Adsorption Kinetics

To gain a better insight into the adsorption mechanism, kinetic of adsorption was assessed because this study is crucial for the practicality of the process. For this study, three various kinetic models were assessed to establish the

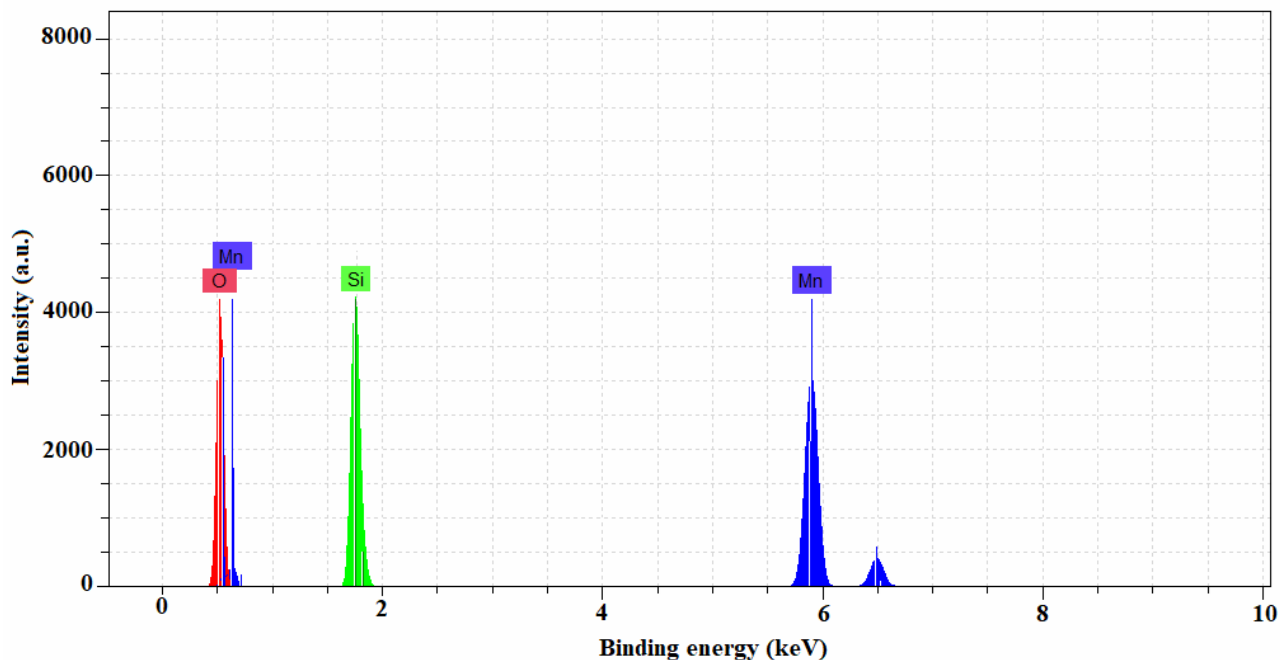


Fig. 3. XPS of Si-MnO<sub>2</sub>.

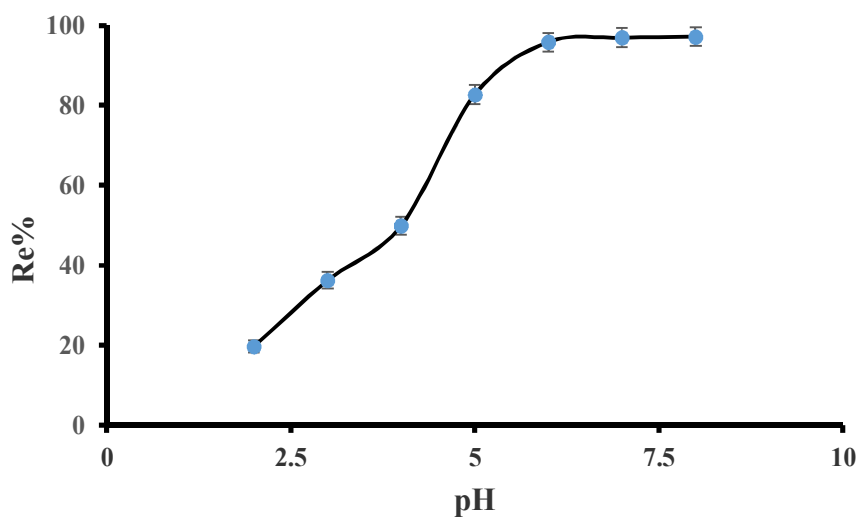


Fig. 4. Impact of pH on MG dye adsorption onto Si-MnO<sub>2</sub>. Conditions: 20 ml MG dye 100.0 mg l<sup>-1</sup>, agitating time: 30 min, agitation velocity: 180 rpm, Si-MnO<sub>2</sub>, 0.05 g.

model with the best fit with experimental data.

Pseudo-first-order kinetic model, Eq. (4), has been often applied in kinetic examinations,

$$\ln (q_e - q_t) = \ln q_e - K_1 t \quad (4)$$

where  $q_e$  and  $q_t$  respectively represent the amounts of MG

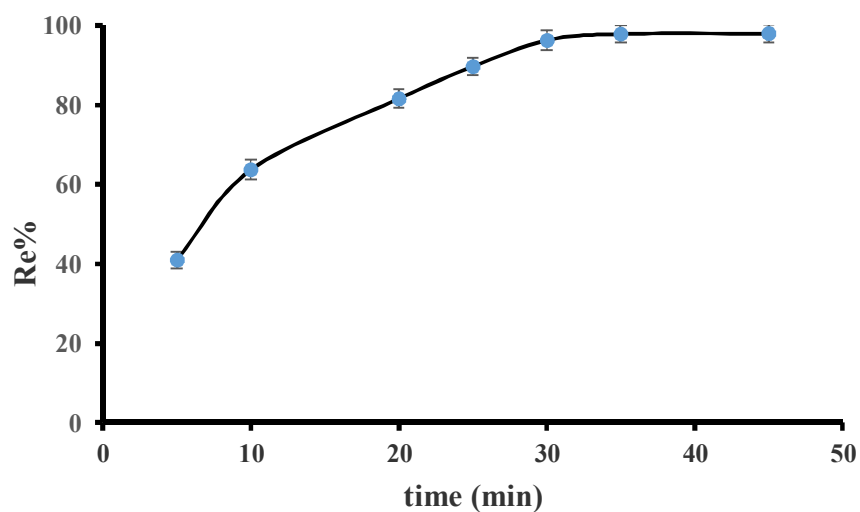


**Fig. 5.** Impact of contact time on MG dye adsorption onto Si-MnO<sub>2</sub>. Conditions are similar to Fig. 4, except for agitation time.

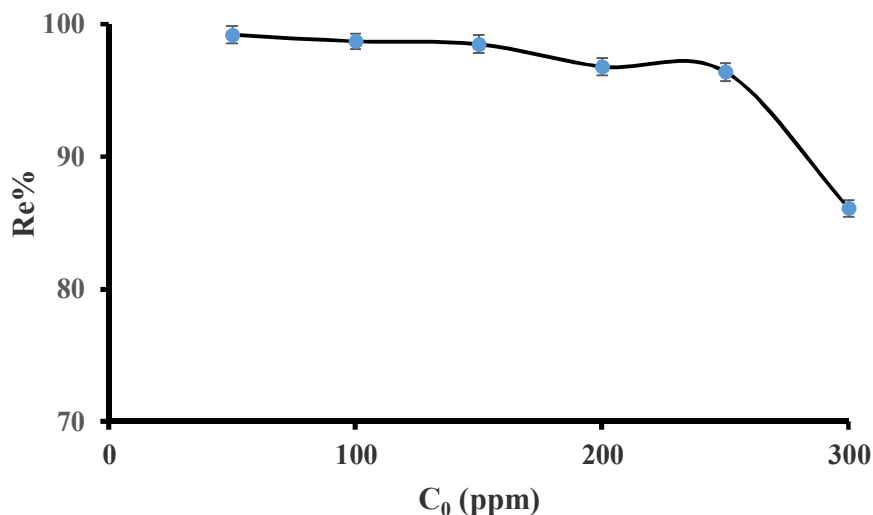


**Fig. 6.** Impact of initial concentrations of MG dye onto Si-MnO<sub>2</sub>. Conditions are similar to Fig. 4, except for initial concentrations.

(mg g<sup>-1</sup>) at equilibrium and at any time, and  $K_1$  is the equilibrium rate constant of pseudo-first-order adsorption (min<sup>-1</sup>). The plot of  $\ln(q_e - q_t)$  vs.  $t$  must provide a linear association and  $K_1$ -value has been identified from the plot slope (Table 2).

The pseudo-second-order kinetic model can be shown by differential Eq. (5),

$$\frac{t}{q_t} = \frac{1}{K_2 q_e^2} + \frac{t}{q_e} \quad (5)$$

where  $K_2$  (g mg<sup>-1</sup> min<sup>-1</sup>) denotes equilibrium rate constant for the pseudo-second-order kinetic model, and may be gained by the plot of  $t/q_t$  vs.  $t$  (Table 2).

Comparing the calculated values of the equilibrium

**Table 1.** Impact of the Initial Concentrations on the MG dye Adsorption onto the Si-MnO<sub>2</sub> Nanocomposite

C <sub>0</sub> (mg l <sup>-1</sup> )	C <sub>e</sub> (mg l <sup>-1</sup> )	q <sub>e</sub> (mg g <sup>-1</sup> )	Removal (%)
50	0.8	19.7	99.2
100	1.3	39.5	98.7
150	1.5	59.4	98.5
200	3.2	78.7	96.8
250	3.6	98.6	96.4
300	13.9	114.4	86.1

**Table 2.** Kinetic Constants for Pseudo-first-order and Pseudo-second-order

Pseudo-second-order			Pseudo-first-order		
R <sup>2</sup>	q <sub>exp</sub>	K <sub>2</sub>	R <sup>2</sup>	q <sub>exp</sub>	K <sub>1</sub>
0.963	35.8	0.005	0.991	49.2	0.144

**Table 3.** Freundlich and Langmuir Constants for MG dye Adsorption onto Si-MnO<sub>2</sub>

Langmuir			Freundlich		
K <sub>L</sub>	b	R <sup>2</sup>	K <sub>t</sub>	1/n	R <sup>2</sup>
0.0093	0.646	0.9987	35.61	0.361	0.875

sorption capacity (Table 2) for various models indicates that pseudo-first-order kinetic model fits best because q<sub>experimental</sub> closely fitted to the experimental value; *i.e.*, 38.5 mg g<sup>-1</sup>.

### Sorption Isotherms

The partitioning of the adsorbate molecules between adsorbent and liquid phase at equilibrium as a function of adsorbate concentration was obtained from the adsorption isotherms. In the present research, the equilibrium results obtained for the removal of MG dye were analyzed using the Langmuir and Freundlich isotherm models.

Langmuir is one of the most widely used isotherm equations for modeling the sorption equilibrium results. The base for Langmuir isotherm is the mono-layer sorption of MG dye on Si-MnO<sub>2</sub> surface. Equation (6) represents linear form of the Langmuir isotherm:

$$\frac{C_e}{q_e} = \frac{1}{K_L b} + \frac{C_e}{K_L} \quad (6)$$

where C<sub>e</sub> (mg l<sup>-1</sup>), q<sub>e</sub> (mg g<sup>-1</sup>), b and K<sub>L</sub>, respectively represent MG concentration in solution, the amount of MG

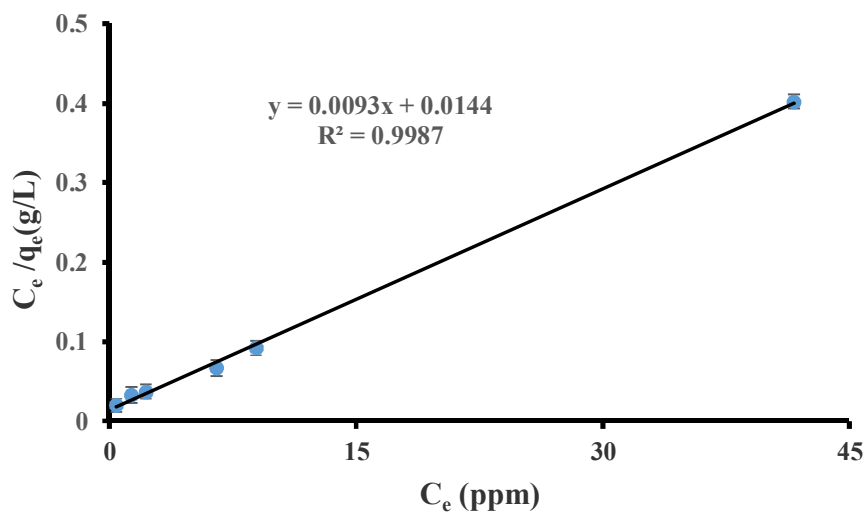


Fig. 7. Langmuir adsorption isotherm of MG dye onto Si-MnO<sub>2</sub> at room temperature.

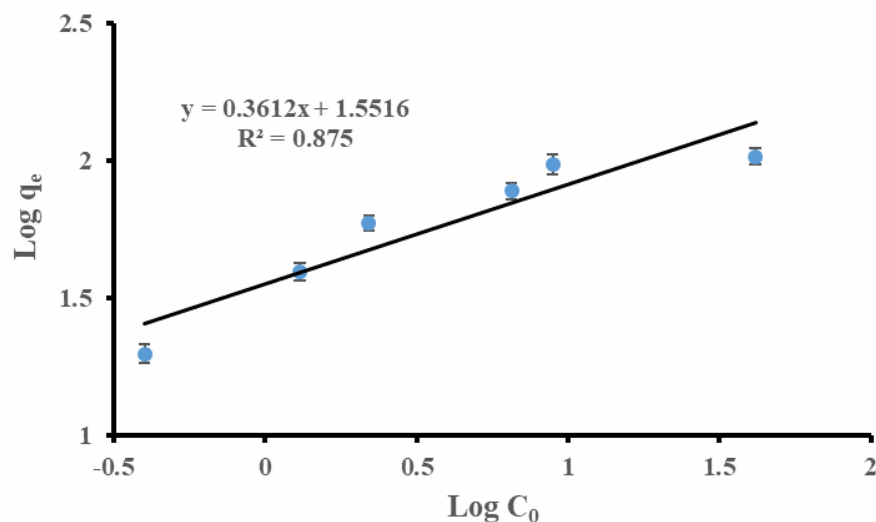


Fig. 8. Freundlich adsorption isotherm of MG dye onto Si-MnO<sub>2</sub> at room temperature.

adsorbed at equilibrium, sorption energy ( $\text{l g}^{-1}$ ) and Langmuir constant ( $\text{mg g}^{-1}$ ). Both  $K_L$  and  $b$  may be specified from a plot  $C_e/q_e$  vs.  $C_e$  (Fig. 7). Table 3 reports  $K_L$ -value,  $b$  constant, and correlation coefficient for the Langmuir isotherm.

The Langmuir isotherm is often assessed *via* a separation factor,  $R_L$  that is defined by Eq. (7):

$$R_L = \frac{1}{1 + bC_0} \quad (7)$$

where  $b$  represents the Langmuir constant and  $C_0$  is the initial concentrations of analyte. The  $R_L$ -value denotes the isotherm form. The  $R_L$ -values between 0 and 1 imply desirable absorption, while  $R_L \geq 1$  or  $R_L = 0$  represent undesirable and irrevocable adsorption isotherms. The calculated  $R_L$ -values at different concentrations (0.005-0.15) are between 0 and 1, denoting a significantly desirable adsorption.

Freundlich isotherm explains heterogeneous surface

**Table 4.** Comparing Adsorption Capacity of Si-MnO<sub>2</sub> with other Sorbents for Removal of MG

Adsorbent	$t_{\text{equilibrium}}$ (min)	$Q^{\circ}$ (mg g <sup>-1</sup> )	Ref.
Activated carbon	25	66.7	[24]
Activated carbon	60	103.6	[32]
Fe <sub>2</sub> O <sub>3</sub> -AC	60	217.7	[32]
Modified chitosan composite	60	4.8	[33]
Activated carbon	4	85.3	[44]
$\gamma$ -Fe <sub>2</sub> O <sub>3</sub> -NPs-AC	4	207	[44]
AC/CoFe <sub>2</sub> O <sub>4</sub> composites	5	89.3	[45]
Ni(OH) <sub>2</sub> -NPs-AC	25	76.9	[46]
Si-MnO <sub>2</sub>	30	107.5	This work

**Table 5.** Thermodynamic Variables for the Adsorption of MG Dye onto Si-MnO<sub>2</sub>

T (K)	$\Delta G^{\circ}$ (kJ mol <sup>-1</sup> )	$\Delta H^{\circ}$ (kJ mol <sup>-1</sup> )	$\Delta S^{\circ}$ (kJ mol <sup>-1</sup> K <sup>-1</sup> )
283	-7.8	28.7	-0.074
293	-6.7		
303	-6.4		
308	-6.1		
313	-5.3		

energy *via* multi-layer sorption. Equation (8) shows linear form of Freundlich isotherm:

$$\log q_e = \log K_f + \frac{1}{n} \log C_e \quad (8)$$

where  $K_f$  and  $1/n$ , respectively represent Freundlich constants (sorption capacity and sorption intensity).  $K_f$  and  $1/n$  may be identified from a plot  $\log q_e$  vs.  $\log C_e$  (Fig. 8). Table 3 reports Freundlich adsorption isotherm constants and correlation coefficient.  $1/n$ -value for Freundlich

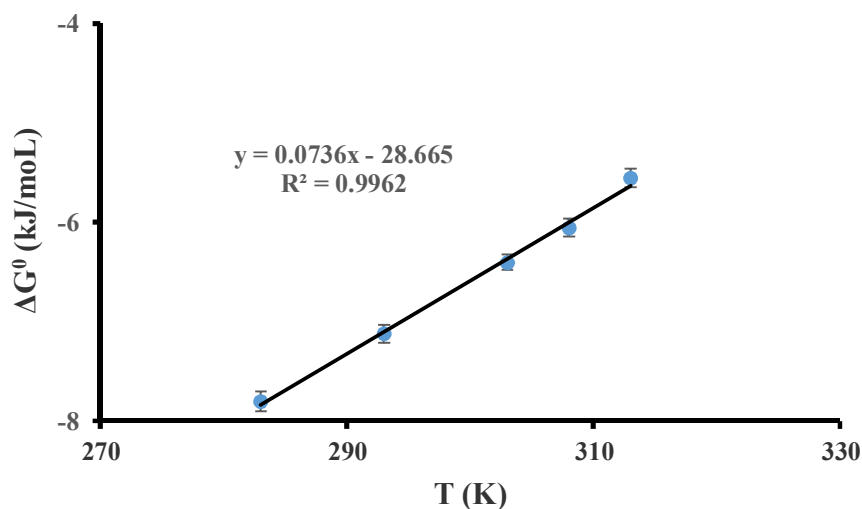


Fig. 9. Thermodynamic study of MG dye adsorption onto Si-MnO<sub>2</sub>.

isotherm has been located between 0 and 1, suggesting that MG dye is well absorbed by Si-MnO<sub>2</sub> at room temperature.

Comparison of the R<sup>2</sup> values (Table 3) for various isotherms indicates that the Langmuir adsorption model provides the best fit since its highest correlation coefficient (R<sup>2</sup> = 0.9987). Therefore, all active sites onto surface of Si-MnO<sub>2</sub> equally adsorb only one molecule, and formed a monolayer with the thickness of a molecule.

### Comparing Adsorption Capacity of Si-MnO<sub>2</sub> with another Sorbents

Mono-layer adsorption capacity for adsorbing MG dye onto Si-MnO<sub>2</sub> compared with other used sorbents [24,32,33,44-46] (Table 4). Comparison indicate that the capacity of Si-MnO<sub>2</sub> (107.5 mg g<sup>-1</sup>) is comparable or higher from other adsorbents, therefore it is a promising adsorbent to remove MG dye from aqueous solutions.

### Thermodynamic Studies

The obtained results from the plot of ΔG° vs. T (Fig. 9) were shown in Table 5. ΔG°-values have been negative, and ΔH° and ΔS° values have been positive. ΔG negative values represent possibility and spontaneous nature of MG adsorption onto Si-MnO<sub>2</sub>. The positive value of ΔH° confirmed that MG adsorption procedure has been naturally endothermic and spontaneous. The positive values of ΔS° showed higher degrees of disorderliness at solid-liquid

interfaces during the adsorption of MG dye onto Si-MnO<sub>2</sub>.

### MG Desorption

The desorption of MG dye from the Si-MnO<sub>2</sub> has been done via shaking them in distinct reagents, including H<sub>2</sub>SO<sub>4</sub>, HNO<sub>3</sub>, and HCl. Findings indicated that desorption of more than 90% of MG dye can be done with 0.1 M HCl solution.

### CONCLUSIONS

This research demonstrates that Si-MnO<sub>2</sub> could be efficiently applied as an adsorbent to remove MG dye from water samples. It was found that the equilibrium results obtained provides the best fit with the Langmuir adsorption model and the maximum mono-layer adsorption capacity for adsorbing MG dye onto Si-MnO<sub>2</sub> was 107.5 mg g<sup>-1</sup>. Figure 5 indicated that MG dye can be quantitatively removed in a very short time. This short time (30 min) to obtain equilibrium is very interesting since equilibrium time is an important parameter for wastewater treatment applications. Adsorption rate and capacity of Si-MnO<sub>2</sub> has been very quick and great in comparison with the other adsorbents used for removing the MG dye from aqueous solution. Being inexpensive, high adsorption rate, high adsorption capability, and reproduction facilities make Si-MnO<sub>2</sub> a good adsorbent for industrial waste waters

treatments.

## ACKNOWLEDGEMENTS

The authors wish to thank Payame Noor University for support of this work.

## REFERENCES

- [1] C. Tamez, R. Hernandez, J. Parsons, *Microchem. J.* 125 (2016) 97.
- [2] E. Sharifpour, H.Z. Khafri, M. Ghaedi, A. Asfaram, R. Jannesar, *Ultrason. Sonochem.* 40 (2017) 373.
- [3] A. Asfaram, M. Ghaedi, G.R. Ghezelbash, *RSC Adv.* 6 (2016) 23599.
- [4] E.A. Dil, M. Ghaedi, G.R. Ghezelbash, A. Asfaram, A.M. Ghaedi, F. Mehrabi, *RSC Adv.* 6 (2016) 54149.
- [5] X. Ma, W. Cui, L. Yang, Y. Yang, H. Chen, K. Wang, *Biores. Technol.* 185 (2015) 70.
- [6] A.A. Bazrafshan, M. Ghaedi, S. Hajati, R. Naghiha, A. Asfaram, *Ecotoxicol. Environ. Saf.* 142 (2017) 330.
- [7] M.T. Yagub, T.K. Sen, S. Afroze, H.M. Ang, *Adv. Colloid Interface Sci.* 209 (2014) 172.
- [8] E. Forgacs, T. Cserhati, G. Oros, *Environ. Int.* 30 (2004) 953.
- [9] S. Karimifard, M.R. Alavi Moghaddam, *Process Saf. Environ. Protect.* 99 (2016) 20.
- [10] J. Luan, P.-X. Hou, C. Liu, C. Shi, G.-X. Li, H.-M. Cheng, *J. Mater. Chem. A* 4 (2016) 1191.
- [11] H. Li, N. An, G. Liu, J. Li, N. Liu, M. Jia, W. Zhang, X. Yuan, *J. Colloid. Interface. Sci.* 466 (2016) 343.
- [12] F. Nasiri Azad, M. Ghaedi, K. Dashtian, S. Hajati, A. Goudarzi, M. Jamshidi, *New J. Chem.* 39 (2015) 7998.
- [13] A. Asfaram, M. Ghaedi, A. Goudarzi, M. Soyak, S. Mehdizadeh Langroodi, *New J. Chem.* 39 (2015) 9813.
- [14] P. Huang, P. Zhao, X. Dai, X. Hou, L. Zhao, N. Liang, *J. Chromatogr. B* 1011 (2016) 136.
- [15] S. Ahad, N. Islam, A. Bashir, S.-U. Rehman, A.H. Pandith, *RSC Adv.* 5 (2015) 92788.
- [16] T. Kamal, M. Ul-Islam, S.B. Khan, A.M. Asiri, *Int. J. Biolog. Macromol.* 81 (2015) 584.
- [17] H. Zheng, J. Qi, R. Jiang, Y. Gao, X. Li, *J. Environ. Manag.* 162 (2015) 232.
- [18] H. Wang, X. Yuan, G. Zeng, L. Leng, X. Peng, K. Liao, L. Peng, Z. Xiao, *Environ. Sci. Poll. Res. Int.* 21 (2014) 11552.
- [19] A. Asfaram, M. Fathi, S. Khodadoust, M. Naraki, *Spectrochim. Acta Part A* 127 (2014) 415.
- [20] M. Dastkhooon, M. Ghaedi, A. Asfaram, A. Goudarzi, S.M. Mohammadi, S. Wang, *Ultrason. Sonochem.* 37 (2017) 94.
- [21] S.Z. Mohammadi, M.A. Karimi, D. Afzali, F. Mansouri, *Cent. Eur. J. Chem.* 8 (2010) 1273.
- [22] S.Z. Mohammadi, H. Hamidian, L. Karimzadeh, Z. Moeinadini, *J. Anal. Chem.* 68 (2013) 953.
- [23] S.Z. Mohammadi, H. Hamidian, Z. Moeinadini, *J. Indust. Eng. Chem.* 20 (2014) 4112.
- [24] S.Z. Mohammadi, M.A. Karimi, S.N. Yazdy, T. Shamspur, H. Hamidian, *Quim. Nova* 37 (2014) 804.
- [25] R. Tabaraki; A. Nateghi, *Anal. Bioanal. Chem. Res.* 5 (2018) 143.
- [26] N.M. Mahmoodi, M. Taghizadeh, A. Taghizadeh, *J. Mol. Liq.* 269 (2018) 217.
- [27] S. Marghzari, M. Sasani, M. Kaykhaii, M. Sargazi, M. Hashemi, *Chem. Cent. J.* 12 (2018) 116.
- [28] W. Qu, T. Yuan, G. Yin, S. Xu, Q. Zhang, H. Su, *Fuel* 249 (2019) 45.
- [29] R.K. Liew, E. Azwar, P.N.Y. Yek, X.Y. Lim, C.K. Cheng, J-H. Ng, A. Jusoh, W.H. Lam, M.D. Ibrahim, N.L. Ma, S.S. Lam, *Biores. Technol.* 266 (2018) 1.
- [30] A. Mohammad Ghaedi, S. Karamipour, A. Vafaei, M. Mehdi Baneshi, V. Kiarostami, *Ultrason. Sonochem.* 51 (2019) 264.
- [31] E. Madrakian, E. Ghaemi and M. Ahmadi, *Anal. Bioanal. Chem. Res.* 3 (2016) 279.
- [32] E. Altıntug, M. Onaran, A. Sari, H. Altundag, M. Tüzen, *Mater. Chem. Phys.* 220 (2018) 313.
- [33] T.K. Arumugam, P. Krishnamoorthy, N.R. Rajagopalan, S. Nanthini, D. Vasudevan, *Int. J. Biol. Macromol.* 128 (2019) 655.
- [34] G. Zhang, L. Shi, Y. Zhang, D. Wei, T. Yan, Q. Wei, B. Du, *RSC Adv.* 5 (2015) 25279.
- [35] H. Altaher, T.E. Khalil, R. Abubeah, *Coloration Technol.* 130 (2014) 205.
- [36] M. Khatami, H.Q. Alijani, B. Fakheri, M.M. Mobasseri, M. Heydarpour, Z.K. Farahani, A. Ullah Khan, *J. of Clean. Prod.* 208 (2019) 1171.

- [37] M. Khatami, R.S. Varma, M. Heydari, M. Peydayesh, A. Sedighi, H. Agha Askari, M. Rohani, M. Baniasadi, S. Arkia, F. Seyedi, S. Khatami, *Geomicrobiol. J.* 36 (2019) 777.
- [38] P. Saharan, A.K. Sharma, V. Kumar, I. Kaushal, *Mater. Chem. Phys.* 221 (2019) 239.
- [39] Goscianska Joanna, Pietrzak Robert, *Catal. Today* 10 (2014) 1016.
- [40] S.R. Srither, A. Karthik, S. Arunmetha, D. Murugesan, V. Rajendran, *Mater. Chem. Phys.* 183 (2016) 375.
- [41] O.A. Elhefnawy, W.I. Zidan, M.M. Abo-Aly, E.M. Bakier, G.A. Al-Magid, *Spectrosc. Lett.* 47 (2014) 131.
- [42] D. Afzali, M. Fayazi, *J. Taiwan Inst. Chem. Eng.* 63 (2016) 421.
- [43] H. Shayesteh, A. Ashrafi, A. Rahbar-Kelishami, *J. Mol. Struct.* 1149 (2017) 199.
- [44] A. Asfaram, Mehrorang, S. Hajati, A. Goudarzi, *Ultrason. Sonochem.* 32 (2016) 418.
- [45] L. Ai, H. Huang, Z. Chen, X. Wei, J. Jiang, *Chem. Eng. J.* 156 (2010) 243.
- [46] S. Agarwal, F. Nekouei, H. Kargarzadeh, S. Nekouei, I. Tyagi, V.K. Gupta, *Process Saf. Environ.* 102 (2016) 85.